Acta Geotechnica (2013) 8:561–565
DOI 10.1007/s11440-013-0238-3

SHORT COMMUNICATION

Extension to barodesy to model void ratio and stress dependency of the K_0 value

Wolfgang Fellin

Received: 29 June 2012 / Accepted: 25 February 2013 / Published online: 19 April 2013

Abstract Barodesy is a new framework for constitutive modelling of soils. The actual version uses a constant value of the coefficient of earth pressure at rest K_0, which contradicts experimental findings. A straightforward modification is presented here to remove this shortcoming. The calibration of the material parameters remains as simple as in the original model.

Keywords Constitutive modelling · Hypoplasticity · Earth pressure at rest

1 Barodesy

Barodesy has been recently invented by Kolymbas [12–15] as a framework for constitutive modelling of soils. Barodesy is mainly based on explicit modelling the asymptotic behaviour of soil [8] which was firsty recognised for sand by Goldscheider [7] and later confirmed, for example, by Chu and Lo [4]. Asymptotic stress paths are reached when soil is deformed with proportional strain paths.[1] This behaviour is modelled by means of a function

$$\mathbf{R}(\mathbf{D}) = \mathbf{I}\,\mathrm{tr}\,\mathbf{D}^0 + c_1 \exp(c_2\mathbf{D}^0), \tag{1}$$

that relates the stretching $\mathbf{D}$ to a tensor $\mathbf{R}$ pointing in direction of the corresponding asymptotic stress path [12]. The stretching $\mathbf{D}$ is the symmetric part of the velocity gradient, and c_1, c_2 are material constants. The superscript 0 denotes the normalisation of a tensor $\mathbf{X}$, i.e. $\mathbf{X}^0 = \mathbf{X}\;|\mathbf{X}|$ with $|\mathbf{X}| = \sqrt{\mathrm{tr}\,\mathbf{X}^2}$. $\mathbf{I}$ is the identity tensor. The stress direction $\mathbf{R}^0$ acts as attractor for any stress path during constant stretching via the evolution equation involving the Jaumann objective stress rate [14]

$$\overset{\circ}{\mathbf{T}} = h \cdot \left(f\mathbf{R}^0 + g\mathbf{T}^0\right) \cdot |\mathbf{D}|. \tag{2}$$

The functions h, f and g are set for sand to [13, 15]

$$h = |\mathbf{T}|^{c_3}\,, \tag{3}$$

$$f = (c_4\,\mathrm{tr}\,\mathbf{D}^0 - c_5 e_c) \exp\left(c_6|\mathbf{R}^0 - \mathbf{T}^0|\right) \tag{4}$$

$$g = c_5 e, \tag{5}$$

with e denoting the void ratio, and e_c the pressure dependent critical void ratio

$$e_c = (1 + e_{c_0}) \exp\left(\frac{|\mathbf{T}|^{1-c_3}}{c_4(1-c_3)}\right) - 1. \tag{6}$$

e_{c_0} is the critical void ratio at zero pressure, and c_3, c_4, c_5 as well as c_6 are additional material constants. The calibration of all material constants is described in [13, 15]. A set of parameters for Hostun RF sand [5] is given in Table 1.

In the special case of isochoric stretching ($\mathrm{tr}\,\mathbf{D} = 0$), the stress directions $\mathbf{R}^0(\mathbf{D})$ belong to critical states and the corresponding asymptotic stress states $\mathbf{T}^0 = \mathbf{R}^0$ are steady states [20]. The critical stress states defined by the R-function (1) of barodesy are practically equal [6] to those modelled by the Matsuoka and Nakai stress criterion [18].

W. Fellin (✉)
Division of Geotechnical and Tunnel Engineering,
University of Innsbruck, Innsbruck, Austria
e-mail: wolfgang.fellin@uibk.ac.at

[1] Proportional strain paths are characterised by constant ratios of the principal values ε_1:ε_2:ε_3, that is, constant ratios of the principal values of the stretching D_1:D_2:D_3.

2 Prediction of K_0

The stress path modelled by (2) for the constant principal stretching D_1 and $D_2 = D_3 = 0$ will approach the proportional stress path $\mathbf{T}^0 = \mathbf{R}^0$, as obtained by the R-function (1)

$$K_0 = \frac{\sigma_3}{\sigma_1} = \frac{R_3}{R_1} = \frac{c_1 - 1}{c_1 \exp(-c_2) - 1}, \tag{7}$$

with σ_1 and σ_3 denoting the major and minor principal stress, respectively. K_0 is predicted to be constant. This contradicts experimental findings, which indicate that K_0 depends on the void ratio or the mean stress or both, for example, [1–3, 9, 16, 17, 19, 22]. Most laboratory experiments indicate that K_0 increases with void ratio. However, recent experiments by Talesnick [19] with stress gauges inside the specimen show the opposite trend. Dynamic compaction of the sample prior to testing may also lead to this opposite behaviour depending on grain-crushing phenomena [17]. It is an open question, which trend is more likely for soils. Both trends can be modelled with the here proposed model via a direct calibration from such experiments. For a more detailed review of other factors influencing K_0 see [9].

3 Extension for void ratio and stress dependent K_0 value

A straightforward approach to model the influence of void ratio and stress level on the K_0 value is to replace the constant c_1 in the R-function (1) by the expression β

$$\mathbf{R}(\mathbf{D}) = \mathbf{I}\,\mathrm{tr}\mathbf{D}^0 + \beta \exp(c_2 \mathbf{D}^0), \tag{8}$$

with

$$\beta = c_1 + c_7(e - e_c). \tag{9}$$

Equation (9) includes the actual void ratio e and the stress level via the pressure dependent critical void ratio (6) and an additional constant c_7.

4 Calibration

The constant c_2 is a function of the critical friction angle solely and can therefore be calibrated as proposed in [14]. The calibration of the constants c_3 and c_4 via fitting the stress-strain response of a loose sample in a oedometric test is negligibly affected if reasonable values for K_0 are chosen. Therefore, the values given in [13, 15] (Table 1) are used here.

The calibration of the material constants c_1 and c_7 follows directly the calibration of c_1 for the original R-function (1) given in [14], which is based on evaluating the peak stress state of a drained triaxial experiment on a dense sample. Using the peak states of experiments with different consolidation pressures and initial void ratios, c_1 and c_7 can be calibrated. In particular, the experiments host-d-triax-cd-600(hfdw09) and host-l-triax-cd-100(hosfl13) from Desrues et al. [5] are used here, see Table 2.

From a peak state, one can evaluate $K_a = \sigma_3/\sigma_1 = (1 - \sin\varphi_p)/(1 + \sin\varphi_p)$ and $\tan\hat{\psi}_p = -1 - (\sin\psi_p + 1)/(\sin\psi_p - 1)$ [14]. Note that $\hat{\psi} := \arctan(-\mathrm{tr}\mathbf{D}/D_1)$ introduced in [14] is just another measurement of the dilatancy. With an arbitrary chosen $D_1 = -1$ follows from the dilatancy $D_2 = D_3 = (\tan\hat{\psi}_p + 1)/2$, hence, the value of β at the peak is

$$\beta_p = \frac{(1 - K_a)\mathrm{tr}\mathbf{D}^0}{K_a \exp(c_2 D_1^0) - \exp(c_2 D_2^0)}. \tag{10}$$

From the stress state at peak $\sigma_3 = \sigma_2 = \sigma_c$ and $\sigma_1 = \sigma_3/K_a$ one can evaluate the critical void ratio at peak $e_{c,p}$ using (6).

The β-function is a linear interpolation between the peak states I and II in Table 2 and therefore

$$c_7 = \frac{\beta_p^I - \beta_p^{II}}{e_p^I - e_{c,p}^I - e_p^{II} + e_{c,p}^{II}} = 4.827 \tag{11}$$

$$c_1 = \beta_p^I - c_7(e_p^I - e_{c,p}^I) = -1.489. \tag{12}$$

Table 1 Material parameters of barodesy for Hostun RF sand

e_{c_0}	c_1	c_2	c_3	c_4	c_5	c_6
0.8703	−1.764	−1.025	0.552	1,174	−3,260	−1.25

From [13, 15]

Table 2 Peak stress states of drained triaxial experiments on Huston RF sand: consolidation stress σ_c, peak friction angle φ_p, angle of dilatancy at peak ψ_p and void ratio at peak e_p

	Experiment from [5]	σ_c (kPa)	φ_p	ψ_p	e_p
I	host-d-triax-cd-600(hfdw09)	−600	38.5°	9.2°	0.6941
II	host-l-triax-cd-100(hosfl13)	−100	34.4°	0.9°	0.8319

$\sin\psi := -\mathrm{tr}\mathbf{D}/(2D_1 - \mathrm{tr}\mathbf{D})$

Table 3 Material parameters of extended barodesy for Hostun RF sand

e_{c_0}	c_1	c_2	c_3	c_4	c_5	c_6	c_7
0.8703	−1.489	−1.025	0.552	1,174	−5,040	−1.25	4.827

e_{c_0}, c_2, c_3, c_4 and c_6 from [13, 15]

Table 4 Peak friction angles φ_p of drained triaxial experiments on dense Hostun RF sand and numerical simulation with original R-function (1) (material parameters from Table 1) and here proposed extended version (8) (material parameters from Table 3)

Test from [5]	Experiment	Original R-function	Extended version
host-d-triax-cd-100(cdhfd11)	44.2°	42.1°	43.9°
host-d-triax-cd-300(hfdw08)	40.7°	39.1°	40.7°
host-d-triax-cd-600(hfdw09)	38.5°	37.6°	38.8°

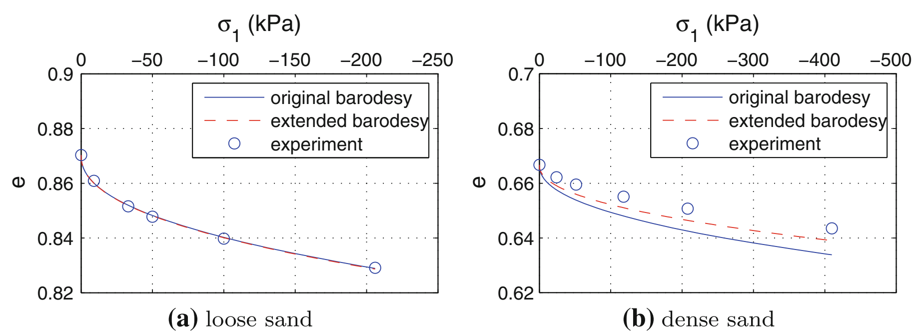

Fig. 1 Oedometric compression on Huston RF sand, initial void ratios: $e_{\text{ini}} = 0.8703$, $e_{\text{ini}} = 0.6667$

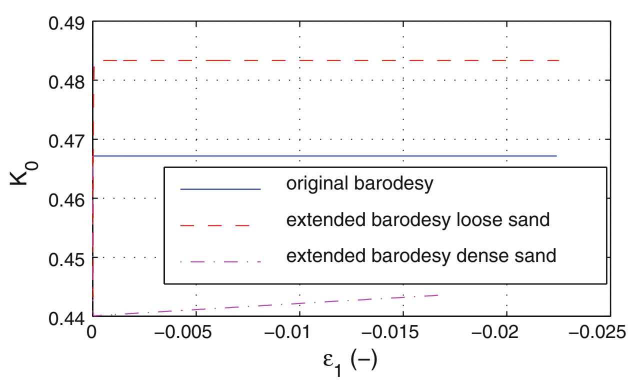

Fig. 2 Oedometric compression on Huston RF sand: $K_0 = \sigma_3/\sigma_1$, with σ_1 and ε_1 the vertical stress and strain, respectively, and σ_3 the horizontal stress

The constant c_5 was calibrated in [13, 15] by fitting the constitutive equation to several experimentally obtained results and c_6 by trial and error. Using the original value of c_5 from Table 2 with the extended form of barodesy yields too small peak friction angles in numerical triaxial test simulations. Decreasing the constant to $c_5 = -5{,}040$ gives good results for the peak friction angles, compare Table 4. The constant c_6 can be left unchanged. The whole set of parameters for Hostun RF sand [5] used here is collected in Table 3.

5 Numerical simulations

Oedometric and triaxial compression test were investigated to highlight the differences between the behaviour of the original and the extended versions of barodesy.

Figure 1a shows the loading branch of the oedometric compression test host-l-oed(Hn2) [5] on loose Huston RF sand (initial void ratio $e_{\text{ini}} = 0.8703$) as well as the computed response for the original and the extended versions of barodesy. As this experiment was used for calibration in [13, 15], the computation with the original model fits quite well. The difference to the computation with the extended model is negligible.

Figure 1b shows the same comparison for the loading branch of the oedometric compression on dense Huston RF sand: host-d-oed(dhn3) [5] (initial void ratio $e_{\text{ini}} = 0.6667$). The extended version of barodesy fits slightly better the experimental results.

The original version of barodesy predicts a constant value of $K_0 = \sigma_3/\sigma_1$. For the parameters in Table 1 and with (7) follows $K_0 = 0.4672$, which is plotted in Fig. 2. The extended version predicts a higher K_0-value for loose samples and a lower one for dense samples, which is in line with experimental observations, for example, [1, 9]. K_0 increases by 9 % for a decrease in e_{ini} of 23 %, which seems to be rather small. A numerical simulation using Hypoplasticity [11] in the version of von Wolffersdorff [21] predicts a similar increase of 8 %. Moreover, K_0 increased in experiments on Karlsruhe sand [10] by 13 % for a decrease in e_{ini} of 29 %.

The empirical equation of Jáky, $1 - \sin\varphi_c$, is widely accepted to predict the K_0 value of normally consolidated clays. The applicability of this relation to sands is questionable since "K_0 of granular materials is not a unique function of neither the critical friction angle nor the peak friction angle [9]". However, in our case $\varphi_c = 33.8°$ [14] and $K_0^{\text{Jáky}} = 0.44$, which is similar to that one predicted by barodesy.

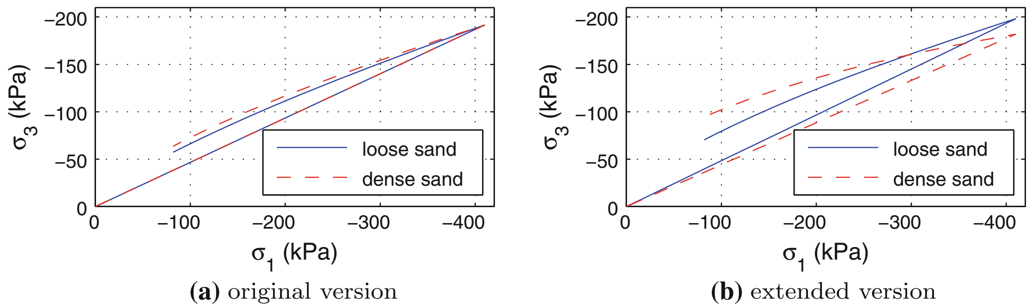

Fig. 3 Oedometric compression and extension on Huston RF sand, initial void ratios: $e_{\text{ini}} = 0.8703$, $e_{\text{ini}} = 0.6667$

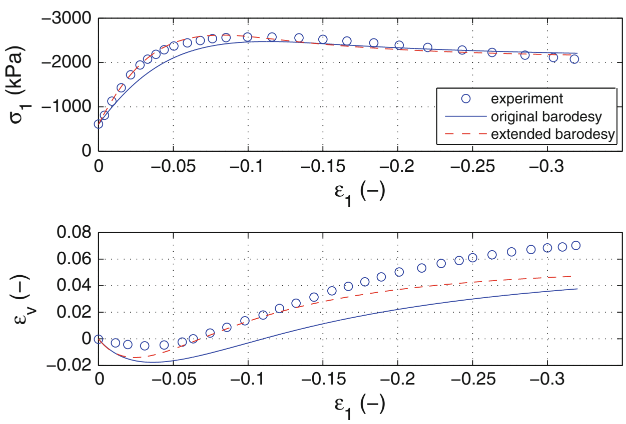

Fig. 4 Triaxial compression on dense Huston RF sand (host-d-triax-cd-600(hfdw09) [5], $e_{\text{ini}} = 0.6707$): σ_1, ε_1 and ε_v are the vertical stress, the vertical and the volumetric strain, respectively; $\sigma_3 = \sigma_2 = 600$ kPa as horizontal stress

The difference between the original and the extended version of barodesy is even more pronounced in oedometric unloading, Fig. 3. The original version predicts only slightly larger pre-loaded state ratios $K = \sigma_3/\sigma_1$ for dense sand than for loose sand. The extended version shows considerable larger differences, which seems to be qualitatively more realistic.

The proposed version is tested on three drained triaxial experiments on dense Hostun RF sand with the consolidation stresses 100, 300 and 600 kPa, see Table 4. The deviation of the numerical peak friction angle to the experimental one is ±1 % in computations with the extended R-function and 2–5 % in computations with the original R-function. Using the extended version allows a slightly better fit of the experimental peak friction angles over the whole experimental stress range. The angle of dilatancy at peak is underestimated with the original version and overestimated with the extended one, see Table 5. The behaviour of both models is exemplified on the numerical simulation of a triaxial test with a consolidation stress of 600 kPa, see Fig. 4. The simulation with the extended version fits slightly better to the experimental data.

Table 5 Angle of dilatancy at peak ψ_p of drained triaxial experiments on dense Hostun RF sand and numerical simulation with original R-function (1) (material parameters from Table 1) and here proposed extended version (8) (material parameters from Table 3)

Test from [5]	Experiment	Original R-function	Extended version
host-d-triax-cd-100(cdhfd11)	16.3°	14.2°	20.1°
host-d-triax-cd-300(hfdw08)	12.5°	10.1°	13.9°
host-d-triax-cd-600(hfdw09)	9.2°	7.6°	10.0°

6 Conclusion

The original version of barodesy assumes a constant value of K_0, which contradicts experimental findings. A straightforward small modification allows for modelling pressure and void ratio dependency of K_0. The additional material constant can be calibrated with triaxial tests on loose and dense samples with different consolidation pressures. Almost all other constants can be used from the original model, with the exception of c_5 which has to be changed slightly. The extended version of barodesy predicts a higher K_0-value for loose samples than for dense samples in keeping with experimental observations. The original version predicts an intermediate value for K_0 and can therefore be seen as reasonable simplification. A slightly better fit of peak friction angles is possible with the extended version.

The extended version may be used in cases when (almost) confined conditions have to be modelled and the stresses evolving due to such a confinement are of interest.

References

1. Bauer E (1992) Zum mechanischen Verhalten granularer Stoffe unter vorwiegend ödometrischer Beanspruchung. Veröffentlichungen des Institutes für Bodenmechanik und Felsmechanik der Universität Fridericiana in Karlsruhe 130
2. Bauer E (1996) Calibration of a comprehensive constitutive equation for granular materials. Soils Found 36(1):13–26

3. Chu J, Gan C (2004) Effect of void ratio on K_0 of loose sand. Géotechnique 54(4):285–288
4. Chu J, Lo SCR (1994) Asymptotic behaviour of a granular soil in strain path testing. Géotechnique 44(1):65–82
5. Desrues J, Zweschper B, Vermeer P (2000) Database for tests on Hostun RF sand. Institutsbericht 13. Institut für Geotechnik, Universität Stuttgart
6. Fellin W, Ostermann A (2011) The critical state behaviour of barodesy compared with the Matsuoka–Nakai failure criterion. Int J Numer Anal Methods Geomech. doi:10.1002/nag.1111
7. Goldscheider M (1976) Grenzbedingung und Fließregel von Sand. Mech Res Commun 3:463–468
8. Gudehus G, Goldscheider M, Winter H (1977) Mechanical properties of sand and clay and numerical integration methods: some sources of errors and bounds of accuracy. In: Gudehus G (ed) Finite elements in geomechanics. Wiley, New York, pp 121–150
9. Guo P (2010) Effect of density and compressibility on K_0 of cohesionless soils. Acta Geotech 5(4):225–238
10. Herle I (1997) Hypoplastizität und Granulometrie einfacher Korngerüste, Veröffentlichung des Institutes für Bodenmechanik und Felsmechanik, vol 142. Universität Fridericiana in Karlsruhe
11. Kolymbas D (1985) A generalized hypoelastic constitutive law. In: Proceedings of the XI international conference on soil mechanics and foundation engineering, San Francisco, Balkema, Rotterdam vol 5, p 2626
12. Kolymbas D (2009) Sand as an archetypical natural solid. In: Kolymbas D, Viggiani G (eds) Mechanics of natural solids, Springer, Berlin, Heidelberg, pp 1–26
13. Kolymbas D (2012a) Barodesy: a new constitutive frame for soils. Géotech Lett 2:17–23
14. Kolymbas D (2012b) Barodesy: a new hypoplastic approach. Int J Numer Anal Methods Geomech 36(9):1220–1240. doi:10.1002/nag.1051
15. Kolymbas D (2012c) Barodesy as a novel hypoplastic constitutive theory based on the asymptotic behaviour of sand. Geotechnik 35(3):187–197
16. Kolymbas D, Bauer E (1993) Soft oedometer—a new testing device and its application for the calibration of hypoplastic constitutive laws. Geotech Test J 16(2):263–270
17. Lirer S, Flora A, Nicotera MV (2011) Some remarks on the coefficient of earth pressure at rest in compacted sandy gravel. Acta Geotech 6(1):1–12
18. Matsuoka H, Nakai T (1974) Stress-deformation and strength characteristics of soil under three different principal stresses. In: Proceedings of JSCE 1974, vol 232, pp 59–74
19. Talesnick M (2012) A different approach and result to the measurement of K_0 of granular soils. Géotechnique 62(11):1041–1045. doi:10.1680/geot.11.P.009
20. Verdugo R, Ishihara K (1996) The steady state of sandy soils. Soils Found 36(2):81–91. http://ci.nii.ac.jp/naid/110003946012
21. von Wolffersdorff PA (1996) A hypoplastic relation for granular materials with a predefined limit state surface. Mech Cohesive Frict Mater 1:251–271
22. Wu W, Bauer E, Kolymbas D (1996) Hypoplastic constitutive model with critical state for granular materials. Mech Mater 23(1):45–69